

N 64 24085

Pulsating Aurorae and Infrasonic Waves in the Polar Atmosphere

KAICHI MAEDA

Code - none

Goddard Space Flight Center, Greenbelt, Md.

AND TOMIYA WATANABE¹

Institute of Earth Sciences, University of British Columbia, Vancouver, Canada

(Manuscript received 1 August 1963, in revised form 24 September 1963)

ABSTRACT

Pulsating aurorae are proposed as a source of the infrasonic waves associated with geomagnetic activity reported by Chrzanowski *et al.* One of the most plausible mechanisms for generating these long period pressure waves is the periodic heating of the upper air around the 100-km level by auroral bombardment, during pulsating visual aurorae. To see the energetic relation between source input and pressure change at sea level, some theoretical calculations are performed with a simple model of auroral distribution in an isothermal atmosphere. At least $100 \text{ erg cm}^{-2} \text{ sec}^{-1}$ of energy flux variation at auroral height is necessary to produce surface pressure amplitudes of the order of 1 dyne cm^{-2} in this model. The intensity of the pressure waves in this model decreases rapidly outside of the region of auroral activity, indicating the importance of sound-ducts in the upper atmosphere for the propagation of these long period sonic waves.

1. Introduction

The purpose of this paper is to interpret the origin of the strange travelling atmospheric waves observed at the ground during intervals of high geomagnetic activity (Chrzanowski *et al.*, 1961). In particular, we seek possible modes of atmospheric oscillations caused by the periodic bombardment of the polar mesosphere by auroral particles.

Trains of these waves are detected by a system of four microphones placed on each corner of a quadrant roughly 8 km square, located north of Washington, D. C. The presence of a travelling wave was established when the same wave forms could be found on all four records, subject to appropriate time shifts between the records. These time displacements were used to determine the direction of wave propagation and the horizontal phase velocity of the waves. The periods of these infrasonic waves are usually from 20 to 80 sec; although occasionally 100- to 300-sec waves are recorded. The pressure amplitude ranges from about one to ten dynes cm^{-2} .

One of the peculiar features of these waves is the change of arrival direction with time of day. They generally come from the northeast in the evening, from north at midnight, and then from the northwest in the morning. The shift back to northeast during the following day is somewhat discontinuous, and they occur less frequently in daytime. Since auroral activity predominates around midnight local time, the time dependence of the appearance of infrasonic waves during intervals of high geomagnetic activity can be explained by as-

suming that the source of this kind of wave is located somewhere in the auroral region, as can be seen from Fig. 1. The left side of this figure shows the diurnal variation of arrival of sound waves during magnetic storms, reported by Chrzanowski *et al.* (1960).

In attempting to understand these peculiar pressure waves, we propose that they originate from a portion of the auroral region, which is heated up periodically by the severe periodic bombardment of auroral particles. As we shall show later, this periodic precipitation of auroral particles is expected to take place simultaneously with the occurrence of geomagnetic pulsations.

2. Inter-relations between geomagnetic fluctuations, pulsating aurorae and infrasonic waves

The auroral luminosity often fluctuates with the fluctuation of incoming auroral particles. The fluctuations of incoming particles, which are mostly electrons, can be explained either by a periodic change in the acceleration mechanism acting on incident particles or by a change of the mirror heights of trapped particles in the earth's atmosphere, following variations in field intensity of the earth's magnetosphere. The variations of geomagnetic field intensity and of auroral brightness are therefore closely related. A clear example of this correspondence between the pulsating aurorae and the rapid variation of geomagnetic intensity observed at the ground was given by Campbell (1960).

Space-probe data have been analyzed by Sonnet *et al.* (1960) and, with data from Explorer X, by Heppner *et al.* (1962, 1963). These results show that the region beyond about ten earth radii near the geomagnetic

¹ This work was supported partly by the Office of Naval Research under Contract No. 3116(00).

equator is occasionally greatly disturbed. Such disturbances may be propagated along the magnetic lines of force as hydromagnetic waves, and are transformed into electromagnetic waves when they reach the conducting ionosphere (Watanabe, 1957, 1962; Piddington, 1959). After penetrating the ionospheric region as electromagnetic waves, they will be almost perfectly reflected at the earth's surface (Sholte and Veldkamp, 1955). This will produce standing hydromagnetic waves along magnetic lines of force. The simplest mode of such standing waves is the fundamental mode, whose single node is on the geomagnetic equatorial plane, with two loops of oscillation on the ends of the line of force on the earth in both hemispheres. This mode of oscillation has been investigated theoretically by Dungey (1954, 1955), who called it the normal mode of torsional oscillations of the magnetic field in the earth's cavity. The eigenperiod of these oscillations increases rapidly as a function of the latitude where the magnetic line of force intersects the earth's surface, varying from several tens of seconds in the subauroral regions to about 10 minutes in the

polar region (Kato and Watanabe, 1956; Obayashi and Jacobs, 1958; Obayashi, 1958).

In addition to the above mode, there is another mode of oscillation responsible for geomagnetic pulsations of shorter periods. As noted by Dessler (1958), the velocity of Alfvén waves in the exospheric region below about 2000 km decreases very rapidly with decreasing height. From continuity of energy flow one can therefore expect Alfvén waves of certain periods coming from the outer exosphere to be intensified. In this mode of oscillation, the layer of maximum Alfvén velocity, which is approximately between 1500 and 3000 km, becomes the node of oscillation, and the loop of oscillation is near the earth's surface. This mode of hydromagnetic oscillation might correspond to the geomagnetic pulsations with periods from about one to several seconds (Jacobs and Watanabe, 1962).

In considering the above facts, one might speculate that a possible mechanism for the production of infrasonic waves during the auroral activity would be the penetration of Alfvén waves, including modified Alfvén

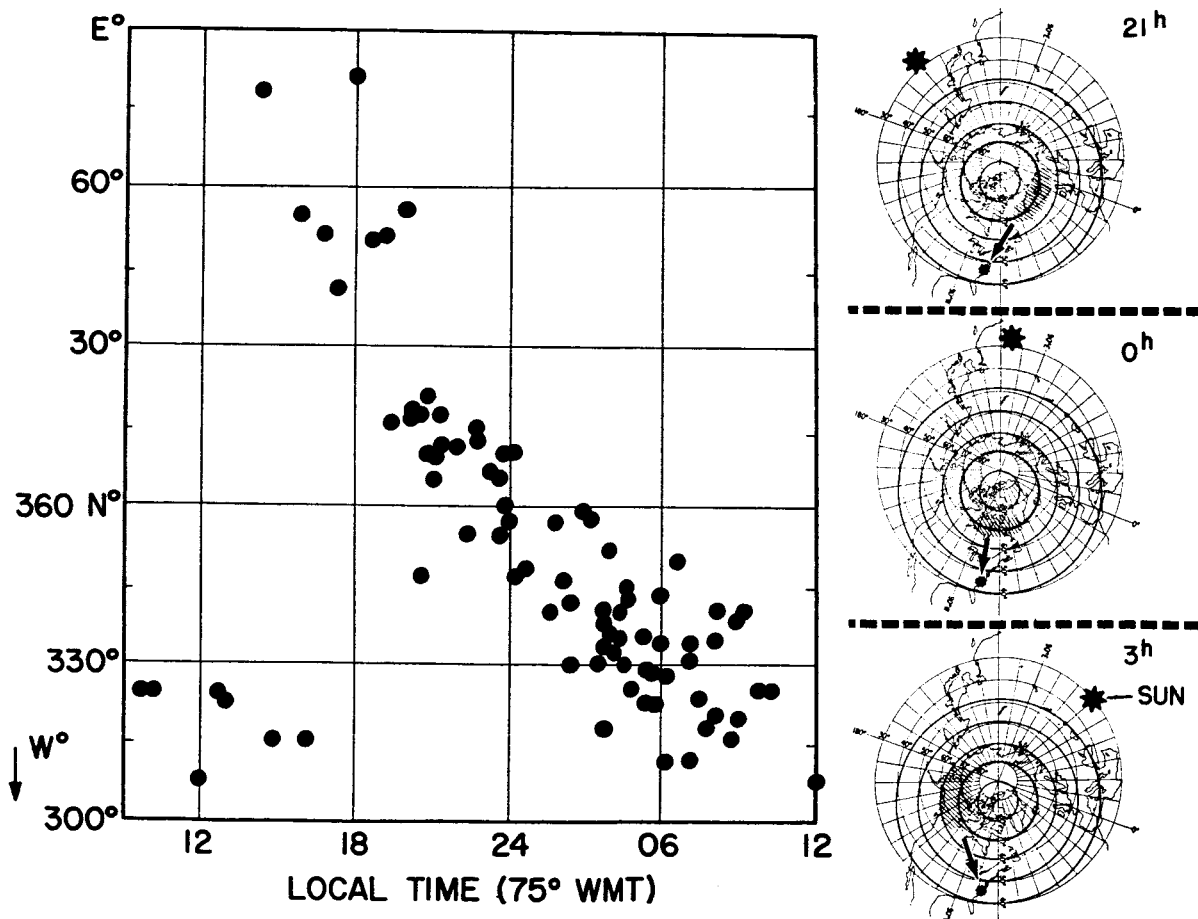


FIG. 1. Diurnal variation of arrival direction of infrasonic waves during magnetic storms observed at the National Bureau of Standards, Washington, D. C. (reproduced from the data reported by Chrzanowski *et al.*, 1961). The three figures on the right side indicate the shifts of the source of these pressure waves, corresponding to the movement of auroral activity. Abscissa is local time at 75° west meridian. (75° WMT).

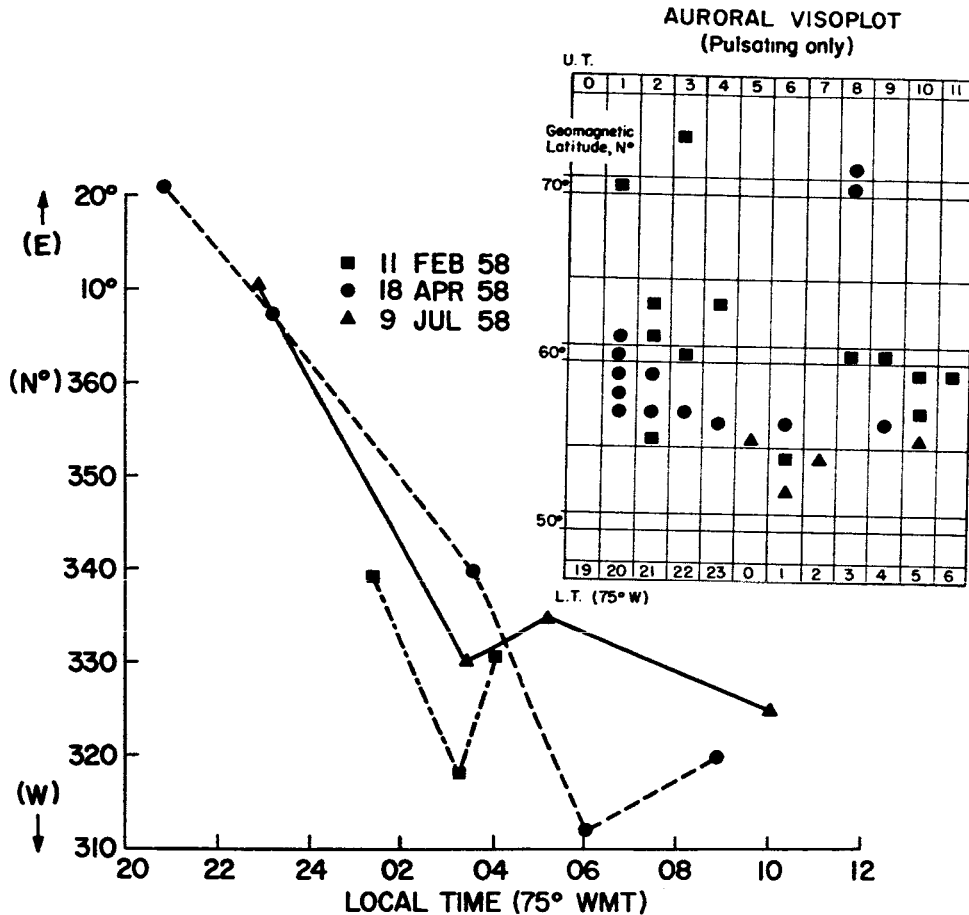


FIG. 2. Diurnal variation of the arrival of infrasonic waves during specific magnetic storms detected at the National Bureau of Standards, Washington, D. C. (Chrzanowski *et al.*), and corresponding auroral activities observed in the northern hemisphere.

waves and retarded sound waves (Obayashi, 1958), through the ionosphere. However, as will be shown later, these contributions are much smaller than the pressure disturbances produced by the periodic heating of the lower ionosphere caused by auroral bombardments.

As shown by Heppner (1954), auroral activity predominates around midnight local time and the active region extends towards lower latitudes with increasing activity, and pulsating aurorae appear at this phase of auroral activity. In other words, among the several types of auroral displays, pulsating aurorae appear with the largest disturbance in energy, and occur in fairly low latitudes. According to Campbell and Rees (1961), the peak of pulsating aurorae is around 100 km, the height of the bottom is 90 km, the effective thickness is of the order of 20 km, and the most frequent period is from 6 to 10 sec. According to the direct measurement of auroral particles by means of rocket-borne detectors, the energy flux of auroral particles (mostly electrons) is of the order of several tens of ergs $\text{cm}^{-2} \text{sec}^{-1}$ for weak aurora. It increases by more than a factor of 50 with

bright aurora (McIlwain, 1960). Thus, one can estimate that the energy flux in strong pulsating aurora is of the order of $10^3 \text{ erg cm}^{-2} \text{sec}^{-1}$, or more. This figure is consistent with the estimate given by Chamberlain (1961) based on measurements of auroral luminosity.

On the other hand, the energy flux of hydromagnetic waves deduced from the magnetic pulsation data is less than $10 \text{ erg cm}^{-2} \text{sec}^{-1}$ at heights below 200 km. The energy flux of hydromagnetic waves increases with height. However, the contribution to pressure waves in the lower atmosphere decreases with increasing height of the source, as will be shown later.

Additional evidence favorable to the present idea is the very good correspondence between the occurrence of pulsating aurorae and infrasonic waves, shown in Fig. 2. The occurrence of pulsating aurorae shown on the right side of this figure is taken from the Visoplot of auroral activity reported from the IGY Data Center, on days which correspond to the events reported by Chrzanowski *et al.* (1961). The latter are shown on the left side of Fig. 2. Strong wind systems at high altitude

may modify the propagation of these sonic waves, and the occurrences of pressure waves do not therefore necessarily match the pulsating auroral events in detail. It is quite clear, however, that there is a close correspondence between the occurrence of infrasonic waves and pulsating aurorae.

3. Mathematical treatment

The excitation and propagation of long-period pressure waves in the atmosphere have been investigated by several workers, mainly in two fields of geophysics, meteorology and ionospheric physics. The theoretical aspects of these problems in geophysics, including oceanography, has been recently reviewed by Eckart (1960). Eckart has developed a mathematical technique to solve these problems, based on the use of modified "field variables" instead of the ordinary hydrodynamical variables. In the present calculations, however, we shall use the classical method, based on the equation for velocity divergence, because of its convenience in comparing the results with observed data. It is obvious that ray theory is not applicable in this problem, because the wavelength of the infrasonic waves is of the order of the "depth" of the atmosphere.

3.1 NOTATIONS AND FUNDAMENTAL EQUATIONS

The notations and constants used are as follows:

$g(0, -g)$	acceleration of gravity, $g=980 \text{ cm sec}^{-2}$;
γ	ratio of specific heats of air, i.e., $C_p/C_v \cong 1.4$, where C_p and C_v are the specific heat of air at constant pressure and volume, respectively;
R	gas constant for air, $B/M=2.87 \times 10^6 \text{ ergs gm}^{-1} \text{ deg}^{-1}$, where B is the universal gas constant, $8.314 \times 10^7 \text{ ergs mol}^{-1} \text{ deg}^{-1}$, and M is the molecular weight of air, approximately 28.97;
Ω	Coriolis vector (=twice the angular velocity of the earth) in rad sec^{-1} ;
\mathbf{f}	resultant of external forces per unit mass except gravity, dyne gm^{-1} ;
$q'(x, z)$	rate of net accession of heat, $\text{erg gm}^{-1} \text{ sec}^{-1}$;
$s(x, z)$	equal to $(\gamma-1)g$, where $q=\rho \cdot q'$ in $\text{erg cm}^{-3} \text{ sec}^{-1}$;
x, z	horizontal (southward) and vertical (upward) coordinates;
$\mathbf{U}(u, w)$	velocity vector, where u is the horizontal (southward) and w is the upward component of air flow in cm sec^{-1} ;
$\chi(x, z)$	the divergence of \mathbf{U} in sec^{-1} , i.e., $\chi=\partial u/\partial x + \partial w/\partial z$;
p', ρ', T'	the small departures from the undisturbed static values of pressure, density, and temperature, functions of x, z , and t ;
p_0, ρ_0, T_0	the undisturbed static pressure, density, and absolute temperature, functions of z only, in dyne cm^{-2} , gm cm^{-3} , and deg K , respectively

p, ρ, T	total pressure, density and temperature, i.e., $p_0+p', \rho_0+\rho'$, and T_0+T' , respectively;
p_s, ρ_s, T_s	static values of pressure, density, and temperature at sea level;
ϕ	specific entropy of air in $\text{erg gm}^{-1} \text{ deg}^{-1}$; $\phi=C_v \ln p - C_p \ln \rho + \text{constant}$
l, λ	vertical and horizontal wavelengths in cm;
τ	period in sec;
k	horizontal wave number corresponding to λ , in cm^{-1} , i.e., $k=2\pi/\lambda$;
σ	frequency, in sec^{-1} , corresponding to τ , i.e., $\sigma=2\pi/\tau$;
D/Dt	the Eulerian derivative, i.e., $\partial/\partial t + \mathbf{U} \cdot \nabla$;
c	velocity of sound in cm sec^{-1} . $c^2=\gamma gH$, where H is the scale height of an isothermal atmosphere, $H=RT/g$.

In the Eulerian notation, the equation of motion is

$$\frac{D\mathbf{U}}{Dt} + \frac{1}{\rho} \nabla p + \mathbf{g} + \Omega \times \mathbf{U} = \mathbf{f}, \quad (1)$$

and the equation of continuity is

$$\frac{D}{Dt} \left(\frac{1}{\rho} \right) - \frac{1}{\rho} \nabla \cdot \mathbf{U} = 0. \quad (2)$$

The variations of pressure caused by thermal excitation can be derived from the first law of thermodynamics, expressed in terms of the change of entropy (Eckart, 1960),

$$\frac{D\phi}{Dt} = \frac{q'}{T}. \quad (3)$$

From the relation $\phi=C_v \ln p - C_p \ln \rho + \text{constant}$, it can be shown that (3) is equivalent to

$$\frac{Dp}{Dt} - \frac{D\rho}{Dt} c^2 = s(x, z, t). \quad (4)$$

Since in our present problem the period of oscillation is less than a few minutes, the Coriolis force due to the earth's rotation is negligible, and all other external forces, except gravity, can be assumed to be zero. The equation of motion for the present problem is then simply written as

$$\frac{D\mathbf{U}}{Dt} + \frac{1}{\rho} \nabla p = \mathbf{g}. \quad (5)$$

3.2 ONE DIMENSIONAL MODEL

For this case the atmospheric motion has only the z -component of velocity, w . The equation of motion (5) is then written in linear approximation by

$$\rho_0 \frac{\partial w}{\partial t} = - \frac{\partial p'}{\partial z} - \rho' g. \quad (6)$$

The equation of continuity is

$$\frac{\partial \rho'}{\partial t} + \rho_0 \frac{\partial w}{\partial z} - \frac{\rho_0}{H} w = 0. \quad (7)$$

The entropy equation (4) can be written in the present case as

$$\frac{\partial p'}{\partial t} = -\rho_0 c^2 \frac{\partial w}{\partial z} + \rho_0 g w + (\gamma - 1) q. \quad (8)$$

$q = q(z, t)$ is the periodically changing heat source. We assume that this varies with z as follows.

$$\text{For } z > 0: \quad q(z, t) = \frac{q_0}{h} e^{-z/h} e^{i\sigma t}. \quad (9)$$

$$\text{For } 0 > z > -z_0: \quad q(z) = 0. \quad (10)$$

q_0 is the maximum rate of heat generation in an atmospheric column with unit cross section. $z = 0$ is taken as the height of the base of the heating, and the earth's surface is given by $z = -z_0$.

By eliminating p' and ρ' from the above equations, the following differential equation is obtained (we consider an isothermal atmosphere):

$$\frac{\partial^2 w}{\partial z^2} - \frac{1}{H} \frac{\partial w}{\partial z} - \frac{1}{c^2} \frac{\partial^2 w}{\partial t^2} = \frac{\gamma - 1}{\rho_0 c^2} \frac{\partial q}{\partial z}. \quad (11)$$

For the region $-z_0 \leq z < 0$, where the heat source is zero, w is given by

$$w = \frac{i}{k_2 - k_1} e^{ik_1 z} A + \frac{i}{k_1 - k_2} e^{ik_2 z} B. \quad (12)$$

For the region $z \geq 0$, w is given by

$$w = \frac{i}{k_2 - k_1} e^{ik_1 z} \left[\int_0^z e^{-ik_1 \xi} Q(\xi) d\xi + C \right] + \frac{i}{k_1 - k_2} e^{ik_2 z} \left[\int_0^z e^{-ik_2 \xi} Q(\xi) d\xi + D \right]. \quad (13)$$

In these expressions k_1 and k_2 are given by

$$k_1 = \sqrt{\frac{1}{l^2} - \frac{1}{4H^2}} - i \frac{1}{2H}, \quad k_2 = -\sqrt{\frac{1}{l^2} - \frac{1}{4H^2}} - i \frac{1}{2H}$$

and Q is given by

$$Q(\xi) = \frac{\gamma - 1}{\rho_0 c^2} \frac{dq(\xi)}{d\xi}.$$

The constants A , B , C and D are to be determined by the following boundary conditions: 1) at $z \rightarrow \infty$, there should be no downward propagating wave, 2) w and p are continuous at the boundary, $z = 0$, and 3) $w = 0$ at the ground, $z = -z_0$.

The pressure variation at the ground is given by (8) with w and $q = 0$:

$$(p')_{z=-z_0} = -\frac{i}{\sigma} \rho_s c^2 \left(\frac{dw}{dz} \right)_{z=-z_0} \quad (14)$$

where ρ_s is the atmospheric density at the earth's surface, i.e., $\rho_s = \rho_0(-z_0)$. Substituting (12) into (14) and making use of the boundary conditions (i) and (ii), we find

$$\left(\frac{dw}{dz} \right)_{z=-z_0} = e^{-ik_1 z_0} \frac{(\gamma - 1) q_0}{\rho_s c^2} \frac{1}{l} \left(1 - \frac{h}{H} + \frac{h^2}{l^2} \right)^{-\frac{1}{2}}, \quad (15)$$

provided that the angular wave frequency σ is larger than a critical frequency σ_A , defined by

$$\sigma_A = \frac{\gamma g}{2c} \quad (16)$$

ρ_s in (15) is the atmospheric density at the height of the base of the heating, i.e., $\rho_s = \rho_0(0)$, and l is the vertical wavelength. Thus, the final expression of the amplitude of pressure variations at the ground, caused by the periodic disturbance in the upper atmosphere $q(z, t)$, is

$$p = \frac{(\gamma - 1)}{c} q_0 \left(\frac{\rho_s}{\rho_c} \right)^{\frac{1}{2}} \left(1 - \frac{h}{H} + \frac{h^2}{l^2} \right)^{-\frac{1}{2}}. \quad (17)$$

The numerical values p/q_0 given by (17) are plotted in Fig. 3 against h (in km) for several values of angular frequency, σ . The full lines and dashed lines represent values based on scale heights of 8 km and 6.8 km, respectively. (The latter gives a proper ratio of $(\rho_c/\rho_s)^{\frac{1}{2}}$ when compared with the observed atmospheric densities.) From this figure, one can see that periodic heating corresponding to a flux of the order of 100 erg cm⁻² sec⁻¹ produces pressure waves with amplitudes of the order of 1 dyne cm⁻² at the ground.

3.3 TWO DIMENSIONAL MODEL

3.3.1 *Equation of velocity divergence.* The equations of motion for the two dimensional case are

$$\rho_0 \frac{\partial u}{\partial t} = -\frac{\partial p'}{\partial x}, \quad (18)$$

$$\rho_0 \frac{\partial w}{\partial t} = -\frac{\partial p'}{\partial z} - g \rho'. \quad (19)$$

The equation of continuity can be written in first order approximation as

$$\frac{\partial \rho'}{\partial t} + w \frac{\partial \rho_0}{\partial z} = -\rho_0 \chi, \quad (20)$$

where $\chi = \chi(x, z, t)$ is the velocity divergence, $\partial u / \partial x + \partial w / \partial z$.

By using (20), (4) can be written as

$$\frac{\partial p'}{\partial t} = \rho_0 g w - \rho_0 c^2 \chi + s. \quad (21)$$

Assuming that the time variations of u , w , p' , ρ' and s are proportional to a factor $e^{i\sigma t}$, we obtain the following relations between u , w and p' from (18)–(21):

$$-\sigma^2 u = \frac{\partial}{\partial x} (c^2 \chi - g w) - \frac{1}{\rho_0} \frac{\partial s}{\partial x}, \quad (22)$$

$$-\sigma^2 w = c^2 \frac{\partial \chi}{\partial z} - \gamma g \chi + g \frac{\partial u}{\partial x} - \frac{1}{\rho_0} \frac{\partial s}{\partial x}, \quad (23)$$

and

$$i\sigma p' = \rho_0 g w - c^2 \rho_0 \chi + s. \quad (24)$$

After eliminating u , w and p from above equations, we obtain the following differential equation for the velocity divergence, $\chi(x, z)$ (Maeda and Watanabe, 1963):

$$\begin{aligned} \nabla^2 \chi + \frac{1}{c^2} \left(\frac{dc^2}{dz} - \gamma g \right) \frac{\partial \chi}{\partial z} - \frac{g}{c^2 \sigma^2} \left(\frac{dc^2}{dz} + (\gamma - 1)g \right) \frac{\partial^2 \chi}{\partial x^2} + \frac{\sigma^2}{c^2} \chi \\ = -\frac{1}{c^2 \sigma^2} \left\{ \frac{g}{\rho_0(z)c^2} \left(\frac{dc^2}{dz} + \gamma g \right) \frac{\partial^2 s}{\partial x^2} - \frac{\sigma^2}{\rho_0 c^2} \left(\frac{dc^2}{dz} + \gamma g \right) \frac{\partial s}{\partial z} - \frac{\sigma^2}{\rho_0} \nabla^2 s \right\}. \end{aligned} \quad (25)$$

3.3.2 The diagnostic diagram. If there is no thermal excitation, the right hand side of (25) is zero, and the solution of this homogeneous differential equation corresponds to free oscillations of the atmosphere (for a flat non-rotating earth).

We now consider pressure waves traveling horizontally in this flat atmosphere. Assuming that u , w , p' , and ρ' are proportional to a factor $e^{i(\sigma t - kx)}$, we get an equation for the vertical change of $\chi(\sigma, z)$.

$$\begin{aligned} \frac{d^2 \chi}{dz^2} + \frac{1}{H} (H' - 1) \frac{d\chi}{dz} \\ + \left[\frac{\sigma^2}{\gamma g H} - k^2 + \frac{k^2 g}{\sigma^2 H} \left(H' + \frac{\gamma - 1}{\gamma} \right) \right] \chi = 0 \end{aligned} \quad (26)$$

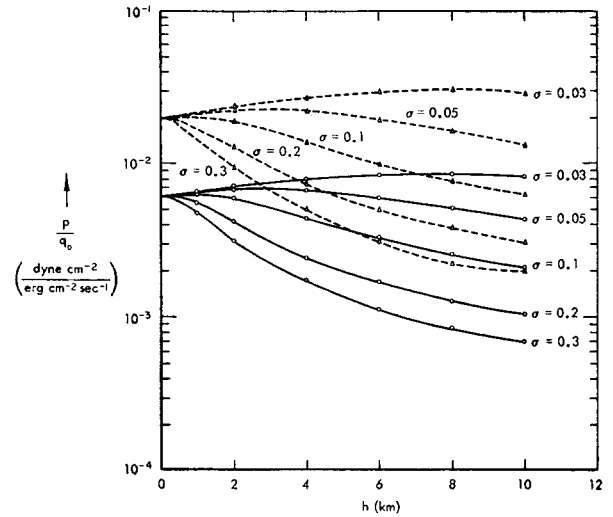


FIG. 3. Relative intensity of (p/q_0) of pressure waves on the ground produced by periodic auroral heating, as a function of the scale height of the heat source, in a one dimensional model of an isothermal atmosphere. (The heating is horizontally uniform.) Full lines and dashed lines correspond to scale heights for an isothermal atmosphere of $H=8$ km and $H=6.8$ km, respectively. The parameter attached to each line is the angular frequency, $\sigma = 2\pi/\tau$, where τ is the period of the wave in sec.

where $H' = dH/dz$, and c^2 has been replaced by $\gamma g H(z)$. For simplicity, let us consider the case of an isothermal atmosphere, where $H' = 0$. Equation (26) reduces to

$$\frac{d^2 \chi}{dz^2} - 2N \frac{d\chi}{dz} + M^2 \chi = 0 \quad (27)$$

where M and N are now constants:

$$N = 1/2H \quad (28)$$

and

$$M^2 = \frac{\sigma^2}{c^2} - k^2 + \frac{k^2 g^2}{c^2 \sigma^2} (\gamma - 1). \quad (29)$$

This differential equation has the following solution:

$$\chi(\sigma, z) = e^{Nz} (A e^{-\mu z} + B e^{+\mu z}) \quad (30)$$

where A and B are constant. The parameter μ is such that

$$\mu^2 = N^2 - M^2 > 0 \text{ for non-cellular solution} \quad (31)$$

and

$$\mu = i\eta, \quad \eta^2 = M^2 - N^2 > 0 \text{ for cellular solution.} \quad (32)$$

As shown by Pekeris (1948), the term with $e^{\mu z}$ must vanish in the non-cellular solution in a single isothermal atmosphere (i.e., $B=0$), otherwise the kinetic energy density, which is proportional to $\rho_0(z)\chi^2$, becomes infinite. The condition that the vertical component of velocity must vanish at the ground then allows only two possible types of free non-cellular oscillation. One corresponds to Lamb's wave (Lamb, 1932, p. 548). It

is non-dispersive ($\sigma = kc$) and exists at all frequencies. The other non-cellular wave can be propagated only above a critical value σ_c , given by

$$\sigma_c = \frac{g}{c} \sqrt{\frac{\gamma}{2}} \quad (33)$$

(the corresponding period is around 250 sec), and is dispersive.

It should be noted that because of the upward decrease of density, the amplitude of the pressure variation in the Lamb wave decreases with altitude by a factor $\exp(-gz/c^2)$, preventing the propagation of these waves in the vertical direction (Eckart, 1960, p. 106).

On the other hand, for the cellular solution, η represents the vertical wave number and (32) is equivalent to

$$\eta^2 c^2 = \frac{(\sigma^2 - \sigma_A^2) + k^2 c^2 (\sigma_B^2 - \sigma^2)}{\sigma^2} \quad (34)$$

σ_A and σ_B are defined as

$$\sigma_A = \frac{g\gamma}{2c}, \quad \sigma_B = \frac{g(\gamma-1)^{1/2}}{c} \quad (35)$$

σ_B is the Brunt frequency.

Brunt's frequency, σ_B , is the frequency of the vertical oscillation of a free air parcel in the atmosphere, changing adiabatically. This expression was also derived by Väisälä as a stability parameter of the atmosphere (Eckart, 1960). σ_A can be called the atmospheric resonance sound frequency (Tolstoy, 1963).

The curve $\eta^2 = 0$ consists of two branches, *A* and *B*,

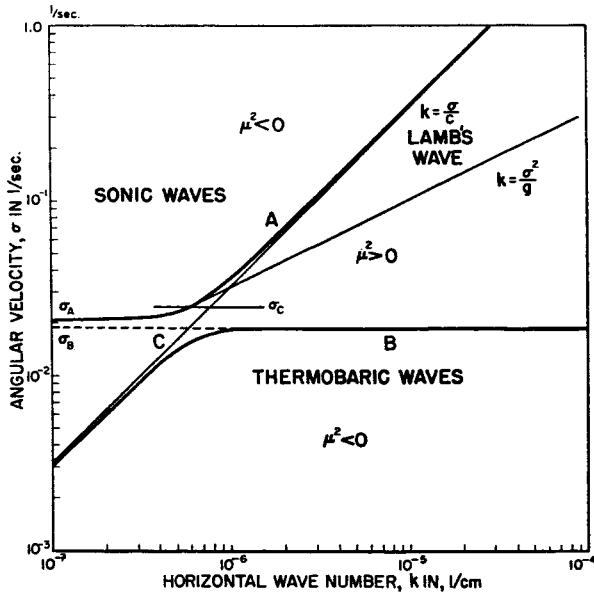


FIG. 4. Diagnostic diagram for an isothermal atmosphere with scale height $H = 8$ km. ($T_0 = 273$ K). See text for meaning of symbols.

as shown in Fig. 4, where σ is plotted against k . The curve *A* starts from the σ -axis at $\sigma = \sigma_A$, and becomes asymptotic to the line *C*, which corresponds to the solution of the non-cellular Lamb wave, $\sigma = kc$. The other curve, *B*, passes through the origin and becomes asymptotic to the horizontal line $\sigma = \sigma_B$.

Following Eckart (1960), Fig. 4 will be called the diagnostic diagram of the isothermal atmosphere, and the waves corresponding to the two domains in which $\eta^2 > 0$ are named as Sonic (mode *A*) and Thermobaric (mode *B*), respectively. Sonic and thermobaric waves are also called acoustic and internal gravity waves, respectively, by Hines (1960).

3.3.3 Intensity of pressure waves at the ground. Since the source of excitation, $s(x, z)$, is assumed to be limited inside the auroral zone, the right hand side of (25) is not uniform with respect to x , and this differential equation is not in general separable with respect to the variables x and z . The following assumptions are therefore made to solve the equation. (i) The atmosphere is isothermal with a constant scale height, H . (ii) The heat source is uniform in the y -direction (this was assumed at the beginning to reduce the problem to two dimensions), but it is limited horizontally in the x -direction to the range $-\lambda_0 \leq x \leq \lambda_0$, and extends vertically above a certain height z_0 . (It is now convenient to have $z = 0$ at the ground.) (iii) The time variation of the heat source is periodic with an angular frequency σ , and of uniform phase within the domain indicated in (ii).

Assumption (i) reduces to the following form:

$$\left(1 - \frac{\sigma_B^2}{\sigma^2}\right) \frac{\partial^2 \chi}{\partial x^2} + \frac{\partial^2 \chi}{\partial z^2} - \frac{1}{H} \frac{\partial \chi}{\partial z} + \frac{\sigma^2}{c^2} \chi = \frac{1}{\rho_0(z)c^2} \left[\left(1 - \frac{g}{\sigma^2 H}\right) \frac{\partial^2 s}{\partial x^2} + \frac{\partial^2 s}{\partial z^2} + \frac{1}{H} \frac{\partial s}{\partial z} \right] \quad (36)$$

Assumptions (ii) and (iii) can be written as

$$s(x, z, t) = s(z) e^{i\sigma t} \theta(z - z_0) [\theta(x + \lambda_0) - \theta(x - \lambda_0)], \quad (37)$$

where

$$s(z) = \frac{(\gamma-1)q_0}{h} \exp\left[-\frac{(z-z_0)}{h}\right], \quad (38)$$

and $\theta(\xi)$ is a unit step-function of ξ , defined by

$$\theta(\xi) = \begin{cases} 1 & \xi \geq 0 \\ 0 & \xi < 0. \end{cases} \quad (39)$$

It should be noted that q_0 is the maximum rate of heat-release in an atmosphere in an air column of unit cross-section, $\text{ergs sec}^{-1} \text{cm}^{-2}$.

Since the atmosphere is assumed to be isothermal, the density of air in equilibrium at height z is given by

$$\rho_0(z) = \rho_0 e^{-z/H}. \quad (40)$$

In order to solve (36) under these conditions the following Fourier transforms are applied with respect to x ,

$$X(k, z) = \frac{1}{\sqrt{2\pi}} \int_{-\infty}^{\infty} e^{ikx} \chi(x, z) dx \quad (41)$$

and

$$S(k, z) = \frac{1}{\sqrt{2\pi}} \int_{-\infty}^{\infty} e^{ikx} s(x, z) dx. \quad (42)$$

Since the heat source $s(x, z)$ vanishes outside of the auroral zone, both $s(x, z)$ and $\chi(x, z)$ must vanish at $x = \pm \infty$. Thus we get

$$\frac{1}{\sqrt{2\pi}} \int_{-\infty}^{\infty} \frac{\partial^2 \chi}{\partial x^2} e^{ikx} dx = -k^2 X(k, z) \quad (43)$$

and

$$\frac{1}{\sqrt{2\pi}} \int_{-\infty}^{\infty} \frac{\partial^2 s}{\partial x^2} e^{ikx} dx = -k^2 S(k, z). \quad (44)$$

Using these transforms, (36) is written as

$$\frac{d^2 X}{dz^2} - 2N \frac{dX}{dz} + M^2 X = F(k, z) \quad (45)$$

where

$$F(k, z) = \frac{1}{c^2 \rho_0(z)} \left[\frac{d^2 S}{dz^2} + \frac{1}{H} \frac{dS}{dz} - k^2 \left(1 - \frac{g}{\sigma H} \right) S \right] \quad (46)$$

and N , M^2 are given in (28) and (29). The total solution of (45) can be written as

$$X(k, z) = e^{n_1 z} \left[C_1 + \frac{1}{2\mu} \int_0^z F(z') e^{-n_1 z'} dz' \right] + e^{n_2 z} \left[C_2 + \frac{1}{2\mu} \int_0^z F(z') e^{-n_2 z'} dz' \right]. \quad (47)$$

n_1 and n_2 are the roots of the characteristic equation

$$n^2 - 2Nn + M^2 = 0, \quad (48)$$

and we write

$$n_1 = N - \mu \quad \text{and} \quad n_2 = N + \mu \quad (49)$$

where μ is given by (31) and (32) for non-cellular or cellular solutions, respectively.

The integration constants C_1 and C_2 are determined by the following two boundary conditions:

1) The vertical component of the velocity vanishes at the ground, i.e.,

$$w(x, z=0) = 0; \quad (50)$$

2) The kinetic energy of the waves at $z = \infty$ is either zero or remains finite. In the latter case, the vertical propagation of the disturbance should be only upwards at $z = \infty$.

The pressure change at the ground can be obtained from $\chi(x, z=0)$, which is given by the inverse Fourier transform of $X(k, z=0)$, i.e.,

$$\chi(x, 0) = \frac{1}{\sqrt{2\pi}} \int_{-\infty}^{\infty} e^{-ikx} X(k, 0) dk \quad (51)$$

where $X(k, 0)$ is the solution of (45) at $z=0$ satisfying the above conditions. It is given by

$$X(k, 0) = \sqrt{\frac{2}{\pi}} \frac{(\gamma-1)q_0}{h\sigma^4 c^2 \rho_0} e^{(z_0/2H) - \mu z_0} \cdot \frac{\sin \lambda_0 k}{k} \cdot \frac{\sigma^4 - k^2 g^2}{(n_1 - m)(n_2 + \beta)} \quad (52)$$

where

$$m(\sigma) = g \left(\frac{\gamma}{c^2} - \frac{k^2}{\sigma^2} \right) \quad (53)$$

and

$$\beta = \frac{1}{h} \frac{1}{H}. \quad (54)$$

Since w and s are zero at the ground, (24) reduces to

$$p'(x, 0) = -\frac{c^2 \rho_s}{i\sigma} \chi(x, 0), \quad (55)$$

with $\chi(x, 0)$ determined by (51)–(54).

TABLE 1. Intensity of cellular mode of infrasonic waves on the ground below the center of the source in units of q_0 for three different periods of the waves, $|p_c|/q_0$.

	$h=H$	$h=\frac{1}{2}H$
$\lambda_0 = 1$ km		
$\tau = 10$ sec	6.75×10^{-6}	1.34×10^{-5}
30 sec	6.28×10^{-5}	1.23×10^{-4}
100 sec	6.92×10^{-4}	1.06×10^{-3}
$\lambda_0 = 10$ km		
$\tau = 10$ sec	1.83×10^{-5}	3.65×10^{-5}
30 sec	4.38×10^{-4}	8.58×10^{-4}
100 sec	6.67×10^{-3}	1.02×10^{-2}
$\lambda_0 = 100$ km		
$\tau = 10$ sec	1.83×10^{-5}	3.65×10^{-5}
30 sec	4.94×10^{-4}	9.67×10^{-4}
100 sec	1.83×10^{-2}	2.83×10^{-2}

TABLE 2. Maximum intensity of non-cellular waves on the ground p_{nc} in units of q_0 , and its ratio to that of cellular waves, $p_{nc}/|p_c|$, for three different periods of the waves. x_0 is the horizontal distance in km of the first nodal lines from the center of the source, the horizontal width of which is assumed to be $\lambda_0 = 10$ km.

	p_{nc}	$p_{nc}/ p_c $	x_0
$h=H$			
$\tau = 10$ sec	1.28×10^{-9}	7.0×10^{-5}	0.85 km
30 sec	3.24×10^{-8}	7.4×10^{-5}	2.56 km
100 sec	1.10×10^{-5}	1.66×10^{-3}	8.30 km
$h=\frac{1}{2}H$			
$\tau = 10$ sec	1.11×10^{-9}	3.03×10^{-5}	0.85 km
30 sec	2.73×10^{-8}	3.18×10^{-5}	2.56 km
100 sec	1.02×10^{-5}	9.8×10^{-4}	8.30 km

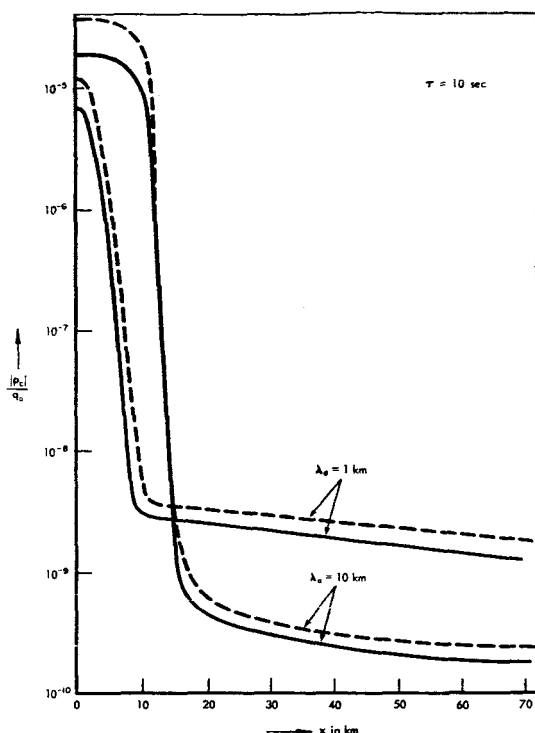


FIG. 5(a). Intensity of cellular waves produced by periodic auroral heating, $|p_c|$ in units of q_0 , as a function of horizontal distance from the center of the source, for wave period $\tau = 10$ sec. Full lines and dashed lines stand for $h = H$ and $h = \frac{1}{2}H$, respectively.

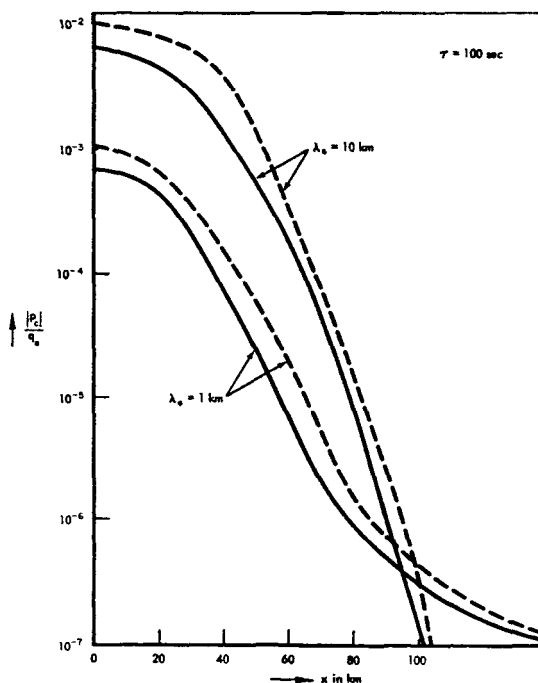


FIG. 5(c). Intensity of cellular waves produced by periodic auroral heating, $|p_c|$ in units of q_0 , as a function of horizontal distance from the center of the source, for wave period $\tau = 100$ sec. Full lines and dashed lines stand for $h = H$ and $h = \frac{1}{2}H$, respectively.

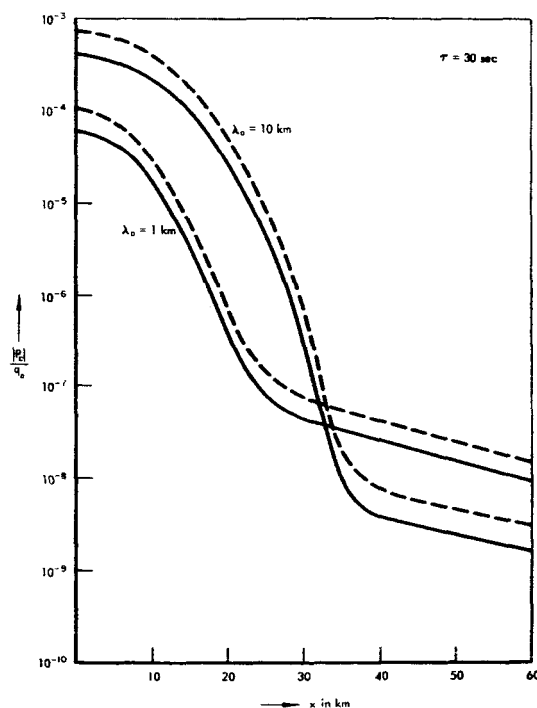


FIG. 5(b). Intensity of cellular waves produced by periodic auroral heating, $|p_c|$ in units of q_0 , as a function of horizontal distance from the center of the source, for wave period $\tau = 30$ sec. Full lines and dashed lines stand for $h = H$ and $h = \frac{1}{2}H$, respectively.

The evaluation of $p'(x, 0)$ is described in the Appendix. Results are shown in Tables 1 and 2, and in Figs. 5 and 6, where p_c and p_{nc} stand for cellular and non-cellular waves, respectively. From these figures, one can see that the sea-level intensity of the infrasonic waves outside of the auroral zone decays rapidly with distance from the source in this isothermal atmosphere.

4. Discussion

4.1 ATTENUATION

Acoustic waves in the atmosphere attenuate because of viscosity and thermal conductivity. The attenuation coefficient, $\alpha(\tau)$ in cm^{-1} , for a wave of period τ is given approximately by (Rayleigh, 1929):

$$\alpha(\tau) = \frac{4\pi^2}{\tau^2} \cdot \frac{1}{c^3} \left[\frac{4}{3} \nu + \frac{\gamma-1}{\gamma} a^2 \right]. \quad (56)$$

The coefficient of kinematic viscosity ν is given approximately by

$$\nu = \frac{1.7 \times 10^{-4}}{\rho(z)} \text{ in } \text{cm}^2 \text{ sec}^{-1} \quad (57)$$

and the coefficient of thermal conductivity a^2 is given by

$$a^2 = \frac{2.1 \times 10^{-5}}{\rho(z)} \text{ in } \text{cm}^2 \text{ sec}^{-1}. \quad (58)$$

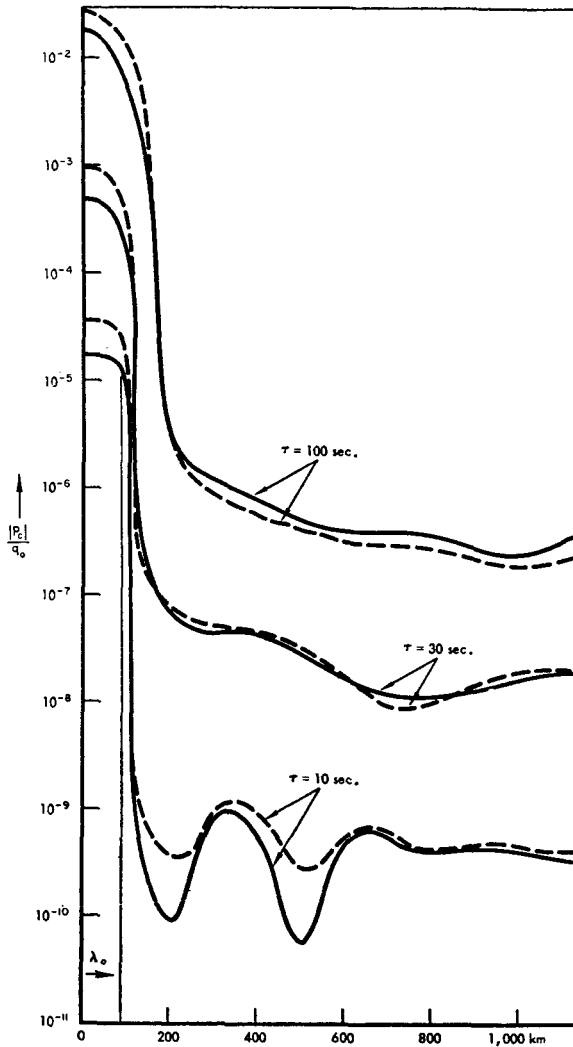


FIG. 6. Intensities of cellular waves on the ground in the units of q_0 as a function of horizontal distance from the center of the source (of width $\lambda_0 = 100$ km), for $\tau = 10$ sec, 30 sec, and 100 sec.

Since the air density ρ decreases exponentially with height, a^2 and ν increase exponentially with altitude. The so-called attenuation factor,

$$f_a(\tau, z) = \exp \left[- \int_0^z \alpha(\tau, z') dz' \right] \quad (59)$$

is shown in Fig. 7 as a function of the height z in km, for $\tau = 10$ sec, 30 sec and 100 sec.

It should be noticed that the relative amplitude of the pressure wave grows with a factor $e^{z/2H}$ as it propagates upward, where H is the scale height, while the absolute amplitude decreases with height by a factor $e^{-z/2H}$, because of the exponential decrease of air density (Schrödinger, 1917). Provided that the amount of excitation energy is the same, therefore, the absolute intensity of the pressure wave at the ground is larger

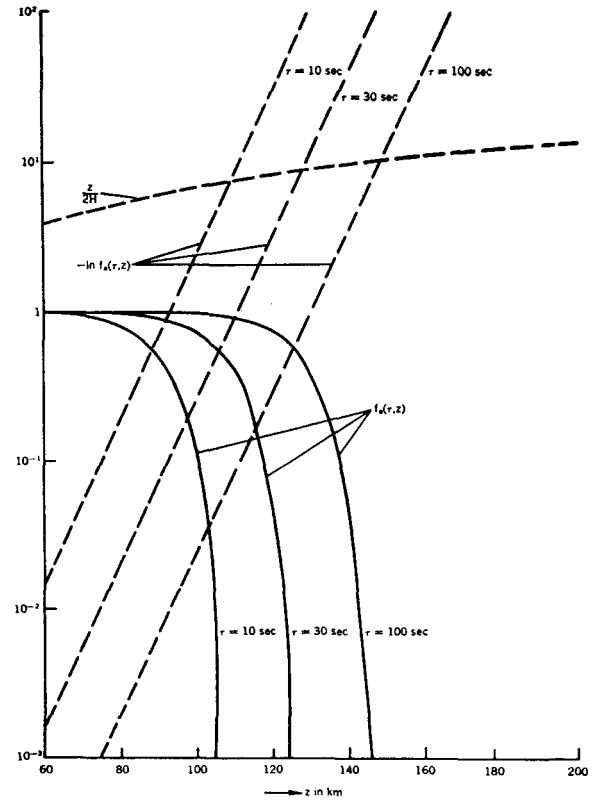


FIG. 7. Attenuation factor $f_a(\tau, z)$ as a function of the altitude z_0 of the source in km (Full lines). Dashed lines indicate $-\ln f_a(\tau, z) = \int_0^z \alpha(\tau, z') dz'$ (straight lines), for $\tau = 10, 30$, and 100 sec and an exponential amplification factor, $\ln(\rho_s/\rho_0)^{1/2} \approx z/2H$, where the scale height, H , is assumed to be 8 km.

when the base of the excitation level is higher. This is shown by (17) and (52) with a factor $e^{z_0/2H}$ for p_s , $p_e(z=0)$ and $p_{nc}(z=0)$, and by a curved dash line in Fig. 7.

However, because of the steep increase of the kinematic viscosity with altitude, the magnitude of the excited pressure wave drops sharply above a certain altitude for a given period (or frequency) of the wave. This is shown in Fig. 8 for three different wave periods $\tau = 10, 30$ and 100 sec. One can see from this figure that there is an effective height of excitation of atmospheric acoustic waves for a given period and that this height increases with period.

4.2 CONDITIONS FOR WAVE FORMATION

According to the calculations in Section 3, the pressure variation at the ground of the order of 1 dyne cm^{-2} can be expected if the maximum rate of heat generation is of the order of 100 erg $\text{cm}^{-2} \text{sec}^{-1}$ and if the layer of periodic heating is around 100 km with a thickness less than 10 km. Electrons with energy of the order of 100 kev will lose most of their energy within a layer of the order of 10 km thickness around the height of 100 km (Chamberlain 1961, p. 290). According to Chamberlain,

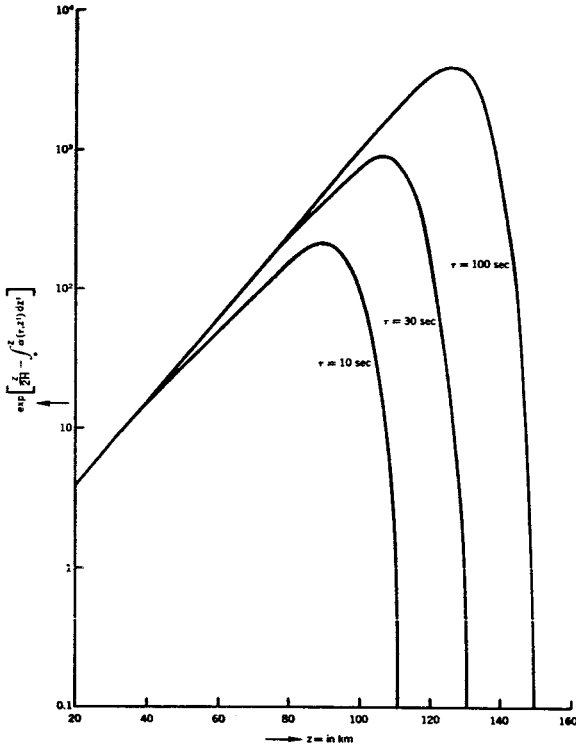


FIG. 8. Relative yield* of the source to the infrasonic waves in the isothermal atmosphere

$$\sqrt{\frac{\rho(z)}{\rho_0}} f_a(\tau, z) \approx \exp \left[\frac{z}{2H} - \int_0^z \alpha(\tau, z') dz' \right]$$

as a function of the altitude of the source (in km), for $\tau = 10$ sec, 30 sec and 100 sec. The scale height H is assumed to be 8 km. (*For a unit intensity of sonic wave occurring at altitude z , the ordinate gives relative intensity of the wave propagated to the ground.)

the rate of heat-generation is the order of $60 \text{ erg cm}^{-2} \text{ sec}^{-1}$ in a bright aurora. Therefore, if the rate of heat-generation changes with this order of amplitude periodically, barometric oscillations of the order of 1 dyne cm^{-2} at sea level can be expected from those sources in the upper atmosphere.

However, several other conditions must be satisfied, in order that the energy brought into the upper air by auroral electrons can be converted efficiently to pressure waves in the atmosphere.

First, the life-time τ_1 of an electron arriving at auroral height from outer space should be smaller than the period, τ , of the waves concerned. If $\tau_1 \gg \tau$, the phase of the time variation of the source differs from place to place, and the resultant pressure wave would be weakened by superposition. Since the auroral electrons, whose velocity is of the order of 10^9 cm sec^{-1} , lose their energy within a layer of 10 km thickness, $\tau_1 \lesssim 10^{-4} \text{ sec}$. This is much smaller than the period of the acoustic waves we consider here.

Electrons impinging into the upper atmosphere lose their energy mostly by inelastic collisions with neutral

air particles until the energy is reduced to $\approx 2 \text{ ev}$, which is the lowest excitation energy of atomic oxygen (1D -state) (Hanson and Johnson, 1960). The time, τ_2 , for 1D excitation collisions with oxygen atoms is of the order of 10^{-3} sec at 100 km and of the order of 1 sec at 400 km. Below 2 ev, the electrons lose energy in the upper atmosphere mainly by elastic collisions with ambient electrons. The time for these low energy electrons to equilibrate with the ambient electrons, τ_3 , is obtained from the expression for the rate of energy loss of a fast electron immersed in a thermalized plasma (Hanson and Johnson, 1960). It is given by

$$\tau_3 \approx 5.7 \times 10^3 E^{1/2} / N_e, \quad (60)$$

where E is the electron energy, i.e., $E \approx 2 \text{ ev}$, and N_e is the electron concentration in cm^{-3} . The equilibration time, τ_3 , given by this expression is about 0.1 sec at 100 km and of the order of 10^{-2} sec above 350 km. Thus $\tau_2 + \tau_3$ is still much smaller than the periods of the acoustic waves under discussion.

It should be noted, however, that elastic collisions with neutral particles dominate over those with ambient electrons below the $F2$ maximum (around 300 km). The time constant, τ_4 for these elastic collisions consists of $\tau(0)$ and $\tau(N_2)$, the time constants for the loss of excess electron energy to atomic oxygen and to molecular nitrogen, respectively, and is given by

$$\tau_4 = \frac{2.08 \times 10^{11} E^{-1/2}}{n(0) + 2.36n(N_2)} \quad (61)$$

$n(0)$ and $n(N_2)$ are the concentration of atomic oxygen and molecular nitrogen per cm^3 , respectively. For $E = 2 \text{ ev}$, τ_4 is of the order of 0.1 sec at 100 km and increases with height. (For example, it is of the order of 100 sec at 350 km.)

As shown in the previous section, the excitation of atmospheric pressure waves above 200 km is not important; and the time constant τ_4 , does not destroy the condition of wave formation. In other words, below 200 km the condition $\tau_1 + \tau_2 + \tau_3 + \tau_4 \lesssim \tau$ is satisfied.

Another condition necessary to wave formation is that the time constant for cooling in a certain domain of auroral activity must be much longer than the period of oscillation. If the initial temperature T_0 is assumed to be horizontally uniform within the source region, $-\lambda_0 \leq x \leq \lambda_0$, then the temperature at the center after $t(\text{sec})$ is, approximately,

$$T(t) = (T_0 - T_a) \Phi \left(\frac{\lambda_0}{2\sqrt{a^2 t}} \right) \quad (62)$$

where

$$\Phi(y) = \frac{2}{\sqrt{\pi}} \int_0^y e^{-x^2} dx \quad (63)$$

a^2 is the thermal diffusivity (coefficient of thermal conduction) of air, and T_a is the temperature outside of the source.

The time, t_a , necessary to reduce the initial temperature difference between the inside and outside of the source region can be estimated by

$$\Phi\left(\frac{\lambda_0}{2\sqrt{a^2 t_a}}\right) = \frac{1}{2} \quad \text{or} \quad t_a \approx \frac{\lambda_0^2}{a^2}. \quad (64)$$

Since the thermal diffusivity at a height $z_0 = 100$ km is of the order of $10^6 \text{ cm}^2 \text{ sec}^{-1}$ (58), the minimum source width needed to satisfy the condition for thermal oscillation is of the order of 30 m for a period of 10 sec, and of the order of 100 m for a period of 100 sec.

The source width considered in our present calculation is significantly larger than these widths. In other words, the time constant for source cooling is sufficiently long for pressure wave production.

4.3 OTHER POSSIBLE MECHANISMS

4.3.1 Periodic heating due to absorption of hydromagnetic waves. As stated in the introduction, hydromagnetic waves from the magnetosphere lose part of their energy in the lower exosphere and in the ionosphere. The remaining energy leaking through the ionosphere is observed as fluctuations of the geomagnetic field intensity, or geomagnetic pulsations.

The rate of energy dissipation of hydromagnetic waves in the ionosphere increases with increasing frequency (Watanabe, 1957; Francis and Karplus, 1960; Akasofu, 1960). According to Watanabe (1957), the dissipation of hydromagnetic wave energy in the ionosphere is negligible for waves with periods longer than 20 sec. In the auroral region, the amplitude of geomagnetic pulsations sometimes exceeds several tens of gamma (i.e., giant pulsations) with periods longer than several tens of seconds. The intensity of the incident wave is usually smaller for higher frequencies (Jacobs and Watanabe, 1962). As shown by the power density of the small scale fluctuations of magnetic field intensity observed in the earth's magnetosphere between 5 and 15 earth's radii (Sonnet *et al.*, 1960), the frequency spectrum of hydromagnetic waves, which are regarded as the origins of geomagnetic pulsations observed at the earth's surface, is a decreasing function of frequencies above the ionosphere. In any case, the upper limit of the incident wave amplitude may be taken as 100γ . The energy flux associated with these hydromagnetic waves is then of the order of several $\text{ergs cm}^{-2} \text{ sec}^{-1}$, assuming that the Alfvén wave velocity above the ionosphere is of the order of 10^8 cm sec^{-1} .

The rate of heat generation by absorption of these hydromagnetic waves in the upper ionosphere has been estimated by several authors (Dessler, 1959; Akasofu, 1960; Francis and Karplus, 1960), and their results are shown in Table 3. The rate of heat generation is generally smaller than $1 \text{ erg cm}^{-2} \text{ sec}^{-1}$, except where the period is 1 sec. Therefore the amount of heat generated by

TABLE 3. Rate of heat-generation due to attenuation of hydromagnetic (HM) waves, with a 100γ incident amplitude

	Period of HM-waves (sec)	Rate of heat generation in air-column (erg sec^{-1} cm^{-2})	Approximate thickness of heating layer (km)	Altitude of the center of heat- generating layer (km)
Dessler (1959)	1	1.3	100	170
Francis- Karplus (1960)	6.3	0.7	50	125
	0.3	1.6	100	180
Akasofu (1960)	1	9.7	100	225
	10	0.17	200	240
	100	0.028	350	250

hydromagnetic waves penetrating the ionosphere is smaller than that due to the auroral particles. Table 3 contains also estimations of the thickness of the layer of heat generation. In every case, the thickness is much larger for hydromagnetic waves than for auroral particles.

As shown in Fig. 8, the effective height of pressure wave generation by periodic heating of the upper air is limited, and is lower for the shorter periods. Therefore, generation of acoustic waves by the attenuation of hydromagnetic waves is less efficient than is generation by the periodic heating due to auroral particles, even if the energy flux of the incident waves is increased to a comparable value.

4.3.2 Pressure waves due to the impacts of auroral particles. A particle coming down into the atmosphere loses its energy by transferring its downward momentum to the air particles. A pressure wave can be generated if the particle flux changes periodically in time. The upper limit of the pressure intensity caused by this process can be estimated by assuming that all the incoming particles would stop in a very short time within a very thin layer. If the average energy of incident electrons is 6 kev and the maximum flux is of the order of $10^{10} \text{ cm}^{-2} \text{ sec}^{-1}$, the maximum pressure thus exerted upon the thin layer acting as a virtual shock absorber is estimated to be of the order of $4 \times 10^{-8} \text{ dynes cm}^{-2}$. The corresponding intensity at the earth's surface would be of the order of $10^{-5} \text{ dyne cm}^{-2}$, if all electrons stop at an altitude of 100 km.

4.3.3 Penetration of hydromagnetic waves through the ionosphere. As mentioned above, many geomagnetic pulsations are due to hydromagnetic oscillations in the exosphere. These oscillations are related to electromagnetic oscillations in the space between the earth's surface and the lower boundary of the ionosphere. Any oscillation mode in which the compression of atmospheric matter is involved gives rise to a variation in the density, and, consequently, a pressure variation. It may thus be possible that geomagnetic pulsations and micro-

barometric oscillations come from the same origin, i.e., hydromagnetic oscillations of the earth's exosphere.

The source of this kind of pulsation is presumably to be found in the outer boundary of the earth's magnetosphere, near the geomagnetic equatorial plane; from there it may be propagated as a modified Alfvén wave. A modified Alfvén wave is a transverse wave with respect to changes in the electric and magnetic fields, while it is a longitudinal wave when viewed as fluid motion (Van de Hulst, 1949). In the space between the earth's surface and the lower boundary of the ionosphere, we should have an electromagnetic wave as well as a pressure wave. The energy flux associated with an incident modified Alfvén wave is roughly $(B^2/8\pi)V_A$, where V_A is the group velocity of the modified Alfvén waves and can be taken as the Alfvén wave velocity at a higher elevation in the ionosphere. B is the amplitude of the wave, i.e., the intensity of magnetic fluctuation above the ionosphere. By assuming conservation of energy flux, we can roughly estimate the upper limit of the amplitude of the pressure wave at the earth's surface, p_s , by the expression

$$\frac{1}{2} \frac{p_s^2}{c_s \rho_s} = \frac{B^2}{8\pi} V_A.$$

c_s is the speed of sound at the earth's surface and ρ_s is the density at the earth's surface. With $V_A = 3.10^7$ cm sec⁻¹, corresponding to day-time conditions at maximum sunspot activity, $B = 30\gamma$, $c_s = 3.10^4$ cm sec⁻¹, $\rho_s = 1.25 \cdot 10^{-3}$ g cm⁻³, we get $p_s \approx 3$ dynes cm⁻².

In this estimate, the conversion factor between the energies of incident Alfvén waves and the secondary pressure waves is assumed to be unity. However, this factor must be very small, because of reflections and dissipations of incident waves at the upper part of the ionosphere. If this factor were not small, one could observe infrasonic waves in equatorial regions during strong magnetic disturbances. Since the occurrence of aurorae in these regions is negligible, this might give a direct detection of modified Alfvén waves coming into the earth's atmosphere from the magnetosphere.

5. Summary

We have shown that one of the most plausible mechanisms for pressure wave generation during geomagnetic disturbances is the periodic heating of the polar ionosphere by auroral particles, observed as pulsating aurorae. As emphasized by Campbell (1962), the main energy source for this type of auroral activity is not only incident auroral particles, but also a flow of secondary electrons, the electro-jet. In this case, periodic heating by these intermittent electric currents is essentially the same as the so-called Joule heating discussed by Cole (1962).

As a result of the present calculations, the following conclusions can be drawn:

- 1) From Figs. 3, 5 and 6, one can see that an incident energy flux of more than 100 ergs cm⁻² sec⁻¹ will produce acoustic waves observable at the ground, provided the periods are longer than about 10 seconds.
- 2) The relative intensity of the pressure wave at the ground is higher when the heating is concentrated within a thin layer than when it is distributed over a wide range of altitude (Figs. 3 and 5).
- 3) The intensity ratio between the inside of the source region and the outside is smaller for longer periods, as expected.
- 4) Similarly, the gradient of intensity around the boundary of the source is steeper when the width of the source is wider.
- 5) The ratio of non-cellular wave intensity to cellular is of the order of 10^{-5} for $\tau = 10$ sec and 10^{-3} for $\tau = 100$ sec, inside of the source. Although the non-cellular intensity exceeds the cellular one at large distances from the source, the contribution of the non-cellular wave to the observed intensity would be negligible, because both waves attenuate in long distance propagation.
- 6) According to the present calculations, *which are based on an isothermal atmosphere*, the intensity of acoustic waves more than several hundred km from the region of auroral activity is negligible. Considering the real atmosphere one is led to conclude, therefore, that the horizontal propagation of acoustic waves through the ducts around the mesopause and the stratopause is rather important to an explanation of the diurnal variation of arrival direction of these waves during the period of high geomagnetic activity (Fig. 1).
- 7) It should be noted, however, that when these sonic waves are observed during periods of magnetic disturbance, auroral activity is not confined within the "auroral zone" but extends toward lower latitudes (nearly to 50N) as can be seen from the auroral visoplots in Fig. 2.

To analyze the position and structure of sonic ducts and the attenuation of the waves, one must take into account the actual atmospheric temperature distribution. This will be discussed elsewhere (Maeda, 1963).

Finally, it should be noted that the energy flux of acoustic waves at the ground S in erg cm⁻² sec is,

$$S = E \cdot c \quad (65)$$

where

$$E = \frac{p^2}{2\rho_s c^2} \quad (66)$$

p and ρ_s are the maximum amplitude of pressure change in dyne cm⁻² and the static density of air at sea level,

respectively, and c is the sound velocity in cm sec^{-1} . Since ρ_s is of the order of $1.25 \times 10^{-3} \text{ g cm}^{-3}$, the energy flux corresponding to $p=1 \text{ dyne cm}^{-2}$ is approximately $1.4 \times 10^{-2} \text{ erg cm}^{-2} \text{ sec}^{-1}$. To see the energy relation between the input power and the observed output intensity, as shown in Figs. 3, 5 and 6, the above relation must be used.

Acknowledgments. The writers wish to express their appreciation to Dr. J. M. Young and his co-workers in the National Bureau of Standards in Washington, D. C., who gave us detailed information on their observations of infrasonic waves during magnetic disturbances. Their thanks are also due Dr. G. D. Mead for his helpful comments, and Mr. E. Monasterski for his kind help with the computer calculations.

REFERENCES

- Akasofu, S., 1960: On the ionospheric heating by hydromagnetic waves connected with geomagnetic micropulsations. *J. atmos. terr. Phys.*, **18**, 160-173.
- Campbell, W. H., 1960: Natural electromagnetic energy below the ELF range. *J. Res. Natl. Bur. Stan.* **64D** (4), 409-411.
- , 1962: Theory of geomagnetic micropulsations. AGU-Annual meeting at Washington, D. C., 28 April 1962.
- , and M. H. Rees, 1961: A study of auroral coruscations. *J. geophys. Res.*, **66**, 41-55.
- Chamberlain, J. W., 1961: Physics of the aurora and airglow. New York, Academic Press, 704 pp.
- Cole, D. K., 1962a: A source of energy for the ionosphere. *Nature*, **194**, p. 75.
- , 1962b: Atmospheric blow-up at the auroral zone. *Nature*, **194**, p. 761.
- Chrzanowski, P., G. Greene, K. T. Lemon and J. M. Young, 1961: Traveling pressure waves associated with geomagnetic activity. *J. geophys. Res.*, **66**, 3727-3733.
- Dessler, A. J., 1958: The propagation velocity of world-wide sudden commencements of magnetic storms. *J. geophys. Res.*, **63**, 405-411.
- , 1959: Ionospheric heating by hydromagnetic waves. *J. geophys. Res.*, **64**, 397-401.
- Dungey, J. W., 1954: The propagation of Alfvén waves through the ionosphere. Ionospheric Res. Sci. Rpt. No. 57, Pennsylvania State Univ., 19 pp.
- , 1955: Electrodynamics of the outer atmosphere. *Report of Physical Society Conference on the Physics of the Ionosphere*, London, Physical Society, 229-236.
- Eckart, H. C., 1960: Hydrodynamics of oceans and atmospheres. New York, Pergamon Press, 290 pp.
- Francis, W. E., and R. Karplus, 1960: Hydromagnetic waves in the ionosphere. *J. geophys. Res.*, **65**, 3593-3600.
- Hanson, W. B., and F. S. Johnson, 1960: Electron temperature in ionosphere. *Memo. Roy. Soc. Sci. Liege*, **4**, 390-423.
- Heppner, J. P., 1954: *A study of relationships between the Aurora Borealis and the geomagnetic disturbances caused by electric currents in the ionosphere*. Ph.D. Thesis, California Institute of Technology. Published as Defence Research Board of Canada, Report No. DR-135, 1958, 39 pp.
- , N. F. Ness, C. S. Scearce and T. L. Skillman, 1963: Explorer 10 magnetic field measurements. *J. geophys. Res.*, **68**, 1-46.
- , N. F. Ness, T. L. Skillman and C. S. Scearce, 1961: Magnetic field measurements with Explorer X satellite. *J. phys. Soc. Japan*, **17**, Suppl. A-2, 546-552.
- Hines, C. O., 1960: Internal atmospheric gravity waves at ionospheric heights. *Canad. J. Phys.*, **38**, 1441-1481.
- Jacobs, J. A., and T. Watanabe, 1962: Propagation of hydromagnetic waves in the lower exosphere and the origin of short period geomagnetic pulsations. *J. atmos. terr. Phys.*, **24**, 413-434.
- Kato, Y., and T. Watanabe, 1956: Further study on the cause of giant pulsations. *Sci. Rep. Tohoku Univ. Ser. 5, Geophysics*, **8**, 1-10.
- Lamb, H., 1932: *Hydrodynamics*. New York, Dover Pub., 738 pp.
- Maeda, K., 1963: The acoustic heating of the polar night mesosphere. NASA Tech. Note, D-1912, 24 pp.; and *J. geophys. Res.*, 1964: **69** (in press).
- , and T. Watanabe, 1963: Infrasonic waves from auroral zone. NASA Tech. Note, D-2138, 41 pp.
- McIlwain, C. E., 1960: Direct measurement of particles producing visible aurorae. *J. geophys. Res.*, **65**, 2727-2747.
- Obayashi, T., 1958: Geomagnetic storms and the earth's outer atmosphere. *Report of Ionos. Res. in Japan*, **12**, 301-335.
- , and J. A. Jacobs, 1958: Geomagnetic pulsations and the earth's outer atmosphere. *Geophys. J.*, **1**, 53-63.
- Pekeris, C. L., 1948: The propagation of a pulse in the atmosphere. Part II, *Phys. Rev.*, **73**, 145-154.
- Piddington, J. H., 1959: The transmission of geomagnetic disturbances through the atmosphere and interplanetary space. *Geophys. J.*, **2**, 173-189.
- Rayleigh, J. W. S., 1929: *The theory of sound*. Vol. II, Cambridge Trans., p. 315.
- Schrödinger, E., 1917: Zur Akustik der Atmosphäre. *Phys. Z.*, **18**, 445-453.
- Sholte, J. G., and J. Veldkamp, 1955: Geomagnetic and geoelectric variations. *J. atmos. terr. Phys.*, **6**, 33-45.
- Sonnet, C. P., D. L. Judge, A. R. Sims and J. M. Kelso, 1960: A radical rocket survey of the distant geomagnetic field. *J. geophys. Res.*, **65**, 55-68.
- Tolstoy, I., 1963: The theory of waves in stratified fluids including the effects of gravity and rotation. *Rev. Mod. Phys.*, **35**, 207-230.
- Van de Hulst, H. C., 1949: Interstellar polarization and magneto-hydrodynamic waves. *Proceedings, Symp. on Cosm. Aerodyn.*, Paris, 45-52.
- Watanabe, T., 1957: Electrodynamical behaviour and screening effect of ionosphere. *Sci. Rep. Tohoku Univ. Ser. 5*, **9**, 81-98.
- , 1962: Law of electric conduction for waves in the ionosphere. *J. atmos. terr. Phys.*, **24**, 117-125.

APPENDIX

Evaluations of $p'(x,0)$

According to (52), $X(k,0)$ is an even function of k . Therefore, the substitution of (52) into (51) gives

$$\chi(x,0) = \frac{2}{\pi} \frac{(\gamma-1)q_0\sigma^2}{hk_0^2\rho_s c^4} e^{x_0/2H} \int_0^\infty \frac{e^{-\mu x_0} \cos xk \sin \lambda_0 k}{k} \cdot \frac{k_0^2 - k^2}{(n_1 - m)(n_2 + \beta)} dk, \quad (\text{A1})$$

where

$$k_g = \frac{\sigma^2}{g}. \quad (\text{A2})$$

μ is a real function of k for $k \geq k_c$ and complex for $0 \leq k \leq k_c$, where

$$k_c = \frac{\sigma}{c} \sqrt{\frac{\sigma^2 - \sigma_A^2}{\sigma^2 - \sigma_B^2}}. \quad (\text{A3})$$

Equation (A1) can then be written as

$$\chi(x, 0) = \chi_c(x, 0) + \chi_{nc}(x, 0) \quad (\text{A4})$$

where

$$\chi_c(x, 0) = -\frac{2}{\pi} \frac{(\gamma-1)q_0\sigma^2}{\hbar k_g^2 \rho_s c^4} e^{z_0/2H} \int_0^{k_c} \frac{e^{-i\eta z_0} \cos xk \sin \lambda_0 k}{k} \cdot \frac{k_g^2 - k^2}{(n_1 - m)(n_2 + \beta)} dk \quad (\text{A5})$$

and

$$\chi_{nc}(x, 0) = -\frac{2}{\pi} \frac{(\gamma-1)q_0\sigma^2}{\hbar k_g^2 \rho_s c^4} e^{z_0/2H} \int_{k_c}^{\infty} \frac{e^{-\mu z_0} \cos xk \sin \lambda_0 k}{k} \cdot \frac{k_g^2 - k^2}{(n_1 - m)(n_2 + \beta)} dk. \quad (\text{A6})$$

The integrand of $\chi_{nc}(x, 0)$ has two singular points, $k_1 = \sigma/c$ and $k_g = \sigma^2/g$, corresponding to the two types of free non-cellular oscillations (Pekeris, 1948). Because of a steep exponential term $e^{-\mu z_0}$, however, contributions of these singularities to the integral is not as important as the contribution from the narrow band near $k \lesssim k_c$, where the exponential term is nearly unity.

The integrand of χ_c has no singularities but oscillates with the factor $e^{-i\eta z_0}$. The main contribution arises also from a narrow domain near $k \lesssim k_c$. Substituting (A4) into (55), we get

$$p'(x, 0) = p_c(x, 0) + p_{nc}(x, 0) \quad (\text{A7})$$

where $p_c(x, 0)$ and p_{nc} correspond to $\chi_c(x, 0)$ and $\chi_{nc}(x, 0)$, respectively.